ORIGINAL RESEARCH

Ferulago angulata activates intrinsic pathway of apoptosis in MCF-7 cells associated with G$_1$ cell cycle arrest via involvement of p21/p27

Hamed Karimian[1]
Soheil Zorofchian
Moghadamtousi[2]
Mehran Fadaeinasab[3]
Shahram Golbabapour[2]
Mahboubeh Razavi[1]
Maryam Hajrezaie[2]
Aditya Arya[1]
Mahmood Ameen Abdulla[4]
Syam Mohan[5]
Hapipah Mohd Ali[2]
Mohamad Ibrahim Noordin[1]

[1]Department of Pharmacy, Faculty of Medicine, [2]Institute of Biological Sciences, Faculty of Science, [3]Department of Chemistry, [4]Department of Biomedical Science, Faculty of Medicine, University of Malaya, Kuala Lumpur, Malaysia, [5]Medical Research Centre, Jazan University, Jazan, Saudi Arabia

Correspondence: Hamed Karimian
Department of Pharmacy, Faculty of Medicine, University of Malaya, 50603 Kuala Lumpur, Malaysia
Tel +603 7967 7520
Fax +603 7967 4964
Email hamedkarimian61@gmail.com

Abstract: *Ferulago angulata* is a medicinal plant that is traditionally known for its anti-inflammatory and antiulcer properties. The present study was aimed to evaluate its anticancer activity and the possible mechanism of action using MCF-7 as an in vitro model. *F. angulata* leaf extracts were prepared using solvents in the order of increasing polarity. As determined by MTT assay, *F. angulata* leaves hexane extract (FALHE) revealed the strongest cytotoxicity against MCF-7 cells with the half maximal inhibitory concentration (IC$_{50}$) value of 5.3±0.82 µg/mL. The acute toxicity study of FALHE provided evidence of the safety of the plant extract. Microscopic and flow cytometric analysis using annexin-V probe showed an induction of apoptosis in MCF-7 by FALHE. Treatment of MCF-7 cells with FALHE encouraged the intrinsic pathway of apoptosis, with cell death transducing signals that reduced the mitochondrial membrane potential with cytochrome *c* release from mitochondria to cytosol. The released cytochrome *c* triggered the activation of caspase-9. Meanwhile, the overexpression of caspase-8 suggested the involvement of an extrinsic pathway in the induced apoptosis at the late stage of treatment. Moreover, flow cytometric analysis showed that FALHE treatment significantly arrested MCF-7 cells in the G$_1$ phase, which was associated with upregulation of p21 and p27 assessed by quantitative polymerase chain reaction. Immunofluorescence and the quantitative polymerase chain reaction analysis of MCF-7 cells after treatment with FALHE revealed an upregulation of Bax and a downregulation of Bcl-2 proteins. These findings proposed that FALHE suppressed the proliferation of MCF-7 cells via cell cycle arrest and the induction of apoptosis through intrinsic pathway.

Keywords: *Ferulago angulata*, apoptosis, cancer, MCF-7, cell cycle, p21/p27

Introduction

Cancer is a debilitating disease that has caused a markedly high death rate in all generations. Despite noteworthy progress in reducing cancer incidence and the developments in chemotherapeutic strategies, it is still a major public health problem in many parts of the world.[1] The available chemotherapeutic agents only provide minimal survival benefits in advanced-stage cancer due to various factors, namely toxicity, side effects, and drug resistance.[2,3] The main modes of therapy used for the treatment of this disease are surgery and chemotherapy, with varying degrees of failure due to high resistance to chemotherapy.[4] Treatment responses are especially gloomy for hormone-independent cancers. Hence, research into new therapeutic agents for these cancers is clearly warranted.[5,6]

Natural products have been used for the treatment of different ailments and diseases for thousands of years.[7,8] Thus, because of the similarity between body composition and plant ingredients and the long history of folk medicine from traditional plants,

there is a rising interest in plant-derived medicines.[9] The World Health Organization estimates that roughly 80% of the world's inhabitants rely on folk medicine for their primary health care.[10] Natural products' contribution to cancer therapy is very evident considering the fact that they were involved in the development of approximately 75% of all novel anticancer agents from 1981–2012.[11,12] Plant products induce cell death by a variety of mechanisms. The most prevalent mechanisms are programmed cell death (PCD)-type I (apoptosis), PCD-type II autophagic cell death, and necrosis.[13]

Apoptosis is a mode of self-cannibalism, which involves individual cells and does not cause inflammation to the neighboring cells.[14,15] Thus, apoptosis, which is characterized by a series of biochemical and morphological changes, including deoxyribonucleic acid (DNA) fragmentation, nuclear condensation, externalization of phosphatidylserine (PS), membrane blebbing, and loss of mitochondrial membrane potential (MMP), has become a mechanism of interest in drug research.[16,17] Mitochondria are found to be a crucial factor in the regulation of apoptosis.[17] A loss in MMP leads to the translocation of proapoptotic Bax to mitochondria, which results in the release of cytochrome *c* and the activation of caspase cascades.[18] In addition, excessive production of reactive oxygen species leading to oxidative stress and the depletion of the glutathione level has been reported to be a trigger to apoptotic signaling.[19,20]

Ferulago angulata, locally known as chavir, is a member of the Apiaceae family, which is mostly indigenous to Iraq, Turkey, and western Iran.[21] This perennial shrub, with a height of ~60–150 cm, is widely used in folk medicine to treat digestive pains, hemorrhoids, snake bites, and ulcers.[22,23] Previous studies have demonstrated antibacterial and antifungal properties of *F. angulata*.[24] The leaves and flowers of this plant showed angiogenesis and migration suppressive effect against human umbilical vein endothelial cells via downregulation of vascular endothelial growth factor-A and vascular endothelial growth factor receptor-2 mRNA expression.[23] In addition, cytotoxic effect of *F. angulata* against K562 and Jurkat cancer cells suggested that this plant has promising anticancer properties.[25,26] Hence, this study was to investigate the anticancer activity of *F. angulata* leaves on the MCF-7 cancer cell line.

Materials and methods
Plant materials
F. angulata plants were collected from Shahrekord, Chaharmahal and Bakhtiari province, Iran, in March 2012,

and a voucher specimen of this plant has been deposited at the Herbarium, Biological Institute, Shahrekord Azad University, Iran. The leaves of *F. angulata* were cut into thin slices and dried at 25°C. The dried leaves (1.5 kg) were then ground with a mill grinder into coarse powder and were first extracted with *n*-hexane (3,000 mL, three times) in conical flasks. The leaves' residues were then dried and sequentially reextracted with dichloromethane and methanol using the same method. The resulting filtrates were dried under reduced pressure by a rotary evaporator (Büchi Labortechnik GmbH, Essen, Germany) at 35°C to produce *n*-hexane (14 g), dichloromethane (10 g), and methanol (9 g) extracts, respectively. The extracts were dissolved in dimethyl sulfoxide (DMSO), (Sigma, St Louis, MO, USA) and stored in −20°C until further experiments.

Cell culture and cell viability assay
A549 (human lung cancer cells), CCD841 (normal human colon epithelial cells), HepG2 (human hepatoma cells), HT29 (human colon cancer cells), MCF-7, and MDA-MB-231 (human breast cancer cells), PC3 (human prostate cancer cells), and WRL-68 (human hepatic cells) cell lines were purchased from American Type Culture Collection (ATCC) (Manassas, VA, USA). The cells were maintained in Roswell Park Memorial Institute 1640 or Dulbecco's Modified Eagle's Medium (Sigma), supplemented with 10% fetal bovine serum (PAA Laboratories GmbH, Pasching, Austria) and 1% penicillin/streptomycin (PAA; 100 μg/mL) in a 37°C incubator with 5% CO_2 saturation. Negative control for all the assays was represented by the untreated medium containing vehicle DMSO (0.1%).

Cell viability was determined using MTT assay. In brief, cells (5×10^4 cells/mL) were treated with three extracts at different concentrations in 96-well plates and incubated for 48 hours at 37°C. MTT was added to the wells and incubated for 3 hours. Cell media was replaced by DMSO and pipetted to dissolve the formed formazan crystals. Then, optical density of the colored solution was quantified at 570 nm wavelength using a microplate reader (UVM340; Asys-Hitech GmbH, Eugendorf, Austria). The potency of cell growth inhibition for each of the three extracts was expressed as an IC_{50} value. MCF-7 cells treated with *F. angulata* leaves hexane extract (FALHE) revealed the lowest IC_{50} when compared to cells treated with the other extracts; therefore, we only used FALHE for further studies. The percentage of cell viability = (absorbance of treated cells/absorbance of untreated cells) ×100%.

Animal experiments and acute toxicity assay

This experiment was carried out after approval by the University of Malaya Institutional Ethics Committee (Ethic #: FAR/26/07/2013/HK [R]). In addition, 6–8 week old rats (150–180 g) were obtained from the Experimental Animal House facility, Faculty of Medicine, University of Malaya. All animals received care, according to the current guidelines for the care of laboratory animals prepared by the National Academy of Sciences and published by the National Institutes of Health Sciences. Also, 18 female rats were divided into three groups and placed in cages that were labeled as: "low dose group" (FALHE, 2 g/kg); "high dose group" (FALHE, 5 g/kg); and "vehicle control group" (Tween-20 10% weight/volume; 5 mL/kg). Before dosing, the rats were fasted overnight but allowed access to water. After fasting, each group was administered with its respective compound, further deprived of food for 3–4 hours, and monitored for 14 days for any sign of toxicity and mortality. Histological, hematological, and serum biochemical parameters were assessed after sacrificing the animals on the 15th day.

Chemical analysis assay

To determine the chemical constituents of FALHE, we carried out the gas chromatography (GC)–mass spectrometry (MS)–time of flight analysis (TOF) analysis, as previously described.[27] The analysis of the FALHE was performed using an Agilent and LECO GC-MS, with the following features: RESTEK, Rxi-5MS capilary column (30 minutes; 0.25 μm film thickness) and a mass spectrometer Pegasus HT High Throughput TOFMS. The carrier gas was helium at a flow rate of 1 mL/minute. Column temperature was initially 40°C for 5 minutes, then gradually increased to 160°C at 4°C/minute, and finally increased to 280°C at 5°C/minute and held for 10 minutes. For GC–MS detection, an electron ionization system was used with ionization energy of 70 eV. The fraction was diluted 1:100 (volume/volume) with ethyl acetate, and 1.0 μL of the diluted sample was injected automatically in splitless mode. The injector temperature was set at 250°C. The detected compounds were identified from their mass spectra by comparison of the retention times of peaks with interpretation of MS fragmentation patterns from data library.

Annexin-V-fluorescein isothiocyanate (FITC) assay

Annexin-V, as a Ca^{2+}-dependent phospholipid-binding protein, detects the plasma membrane alterations, such as the PS externalization during the early stages of apoptosis.[28] The effect of FALHE on the induction of early apoptosis was analyzed in MCF-7 cells using the annexin-V probe. The MCF-7 cells (5×10^4 cells/mL) at the exponential phase of growth were seeded into a chamber slide plate. After 48 hours of FALHE treatment at IC_{50} doses, they were washed with phosphate buffered saline (PBS) and stained with fluorescein-labeled annexin-V containing a binding buffer. The MCF-7 cells were observed under fluorescent microscopy, Olympus BX51 (Olympus Corporation, Tokyo, Japan).

To confirm PS translocation suggesting an induction of apoptosis by FALHE observed in microscopic investigation, we carried out the flow cytometric analysis using the BD Pharmingen Annexin V-FITC Apoptosis Detection Kit (APOAlert® Annexin V; Clontech, Mountain View, CA, USA). In brief, MCF-7 cells (1×10^5 cells/mL) at the exponential phase of growth were exposed to FALHE at IC_{50} concentration for 24, 47, and 72 hours. After centrifuging the cells and removing the media, the MCF-7 cells were washed twice with PBS and resuspended in the annexin-V binding buffer. The cells were then stained with annexin-V-FITC and propidium iodide (PI), according to the manufacturer's instructions. The flow cytometric analysis was performed using BD FACSCanto II flow cytometer (BD Biosciences, San Jose, CA, USA) followed by quadrant statistics analysis for the detection of early and late apoptotic cells and necrotic cells.

Cell cycle analysis

Cell cycle analysis was carried out using a flow cytometer as previously described.[29] In brief, the MCF-7 cells (5×10^4 cells/mL) at the exponential phase of growth were treated with FALHE for 24, 48, and 72 hours. After incubation, treated MCF-7 cells were centrifuged and washed with PBS twice prior fixing with 95% cold ethanol (700 μL) at 4°C overnight. After fixing, the cells were washed again and resuspended in PBS (500 μL). The fixed MCF-7 cells were treated with PI (80 μL; 1 mg/mL) for 45 minutes, and the binding ability of PI was restricted to DNA by adding the ribonuclease A (20 μL; 10 mg/mL) for degradation of RNAs. The DNA content of the cells was analyzed by using a BD FACSCanto II flow cytometer (BD Biosciences, San Jose, CA, USA) and a ModFit LT software (Verity Software House, Inc., Topsham, ME, USA).

Caspase analysis

The effect of FALHE on the activation of caspase-8 and caspase-9 was investigated using a commercial kit

(Caspase-Glo 8 assay and Caspase-Glo 9 assay; Promega Corporation, Fitchburg, WI, USA), as previously described.[6] In brief, the MCF-7 cells (2×10^4 cells/well) were plated in white-walled 96-well plate and treated with IC_{50} doses of FALHE for 3, 6, 12, 24, 48, and 72 hours. After the incubation time, Caspase-Glo Reagent -8 and -9 (50 μL) was added to each well and incubated for 30 minutes in the dark. The activation of the caspases was investigated using a luminescence microplate reader (Infinite M200PRO; Tecan Schweiz AG, Männedorf, Switzerland).

Multiple cytotoxicity assay

Multiple cytotoxicity was determined using the Cellomics Multiparameter Cytotoxicity 3 Kit (Cellomics, Pittsburgh, PA, USA), as previously described in detail.[30] This kit provides simultaneous measurements of four independent cell health parameters in a single cell, ie, changes in nuclear intensity, cell membrane permeability, cytochrome c release, and MMP. In this experiment, MCF-7 cells were stained with the nuclear dye (Hoechst 33342), cell permeability dye (FITC), mitochondrial membrane potential dye (Cy5), and cytochrome c dye (Cy3). The plates were analyzed using the ArrayScan HCS system (Cellomics).

Apoptosis proteome profiler array

To determine the probable mechanism of action for induced apoptosis by FALHE, we examined the proteins involved in different pathways of apoptosis using the Proteome Profiler Array (RayBio Human Apoptosis Antibody Array Kit, RayBiotech, Inc., Norcross, GA, USA), according to the manufacturer's protocol. Briefly, after treatment of MCF-7 cells with FALHE at IC_{50} dose for 48 hours, the proteins were extracted from each sample, and 300 μg of the extracted proteins were incubated with the human apoptosis array for 24 hours. The membrane was then used to quantify the result via scanning on a Biospectrum AC ChemiHR 40 (UVP, Upland, CA, USA). An image analysis software (Progenesis SameSpots software v.2.0.2733.19819; Nonlinear Dynamics, Newcastle, UK) was used to analyze the array image file.

Gene expression analysis of Bax/Bcl-2 and p21/p27

The gene expression of four proteins, namely Bax, Bcl-2, p21, and p27, which demonstrated the highest changes in proteome profiler array when compared to the control, was investigated by quantitative polymerase chain reaction analysis. After treatment of MCF-7 cells with FALHE

at an IC_{50} dose for 24, 48, and 72 hours, total RNAs were isolated using a Quick-RNA MiniPrep kit (Zymo Research, Freiburg, Germany), followed by the synthesization of complementary DNAs using a High-Capacity RNA-to-cDNA kit (Applied Biosystems, Foster City, CA, USA), according to the manufacturer's instructions. The gene expression was measured, based on the relative expression of β-actin as a positive reference. Applied Biosystems StepOnePlus system (Applied Biosystems), Solaris qPCR Gene Expression Master Mix and Solaris Gene Expression (Thermo Fisher Scientific, Waltham, MA, USA) Assays were used for the gene expression analysis of: Bcl-2, AX-003307-00-0100; Bax, AX-003308-00-0100; p21, AX-003471-00-0100; p27, AX-003472-00-0100; GAPDH, AX-004253-00-0100; and β-actin, AX-003451-00-0100.

Immunofluorescence analysis of Bax/Bcl-2

To determine the changes in the expression of Bax and Bcl-2 at the protein level, immunofluorescence analysis was carried out using the Cell Reporter™ (Molecular Devices, Wokingham, UK).[31] The MCF-7 cells (5×10^3 cells/well) at the exponential phase of growth were seeded in 96-well plate and treated with FALHE at IC_{50} dose for 24, 48, and 72 hours. After incubation, the cells were fixed using 4% paraformaldehyde at 25°C for 15 minutes. Then, each well was supplied with blocking buffer (0.03% Triton X-100/ PBS and normal serum) for 1 hour. After blocking, the cells were treated with diluted primary antibody solution (1× PBS; BSA/0.3% Triton X-100) and incubated overnight at 4°C. Bax and Bcl-2 fluorochrome-conjugated secondary antibodies (Santa Cruz Biotechnology, Santa Cruz, CA, USA) were diluted in PBS and added to each well and incubated for 1 hour at room temperature. Cells were treated with 4′,6-diamidino-2-phenylindole (DAPI) and examined using the Cell Reporter™ cytofluorimetric system. During the process, cells were washed twice with PBS after every single step.

Statistical analysis

Each assay was carried out three times independently. Statistical analysis was performed using the statistical package GraphPad Prism Version 5 (GraphPad Software Inc., San Diego, USA) and the SPSS-16.0 package (SPSS Inc., Chicago, IL, USA, USA). One-way analysis of variance (Dunnett's multiple comparison test) was used to distinguish the difference among groups. The results are presented as the means ± standard error of the mean of three

independent experiments. *$P<0.05$ was considered statistically significant.

Results and discussion

Cytotoxic effects of FALHE on different cancer cells

The cytotoxic effects of three *F. angulata* extracts on different cancer cells were determined using the MTT assay. Dichloromethane and methanol extracts did not show significant cytotoxic effect toward cancer cells compared to the hexane extract. Meanwhile, the FALHE treatment of cancer cells for 48 hours decreased cell proliferation with a wide range of suppressive effects (IC_{50} ranged from 5.3±0.82 to 70.25±7.42 µg/mL), due to the various range of resistance shown by cancer cells. As shown in Figure 1A, FALHE

elicited the strongest cytotoxicity effect on the MCF-7 cells with the IC_{50} value of 5.3±0.82 µg/mL at 48 hours.

In addition, the suppressive effect of FALHE on MCF-7 cells was proved to be concentration- and time-dependent (Figure 1B). In contrast, even the highest concentration of FALHE (50 µg/mL) did not significantly affect the proliferation of normal cells (WRL-68 and CCD-841). The cell viability implied FALHE's suppressive effect is selective for cancer cells. Following these results, MCF-7 cells and FALHE were chosen for subsequent experiments. Findings from this study were comparable with a previous study, which showed significant cytotoxic effects of *F. angulata* against the Jurkat cell line ($IC_{50} <8$ µg/mL).[25] However, an investigation on its suppressive effect on Raji (B-cell lymphoma), U937 (human leukemic monocyte lymphoma),
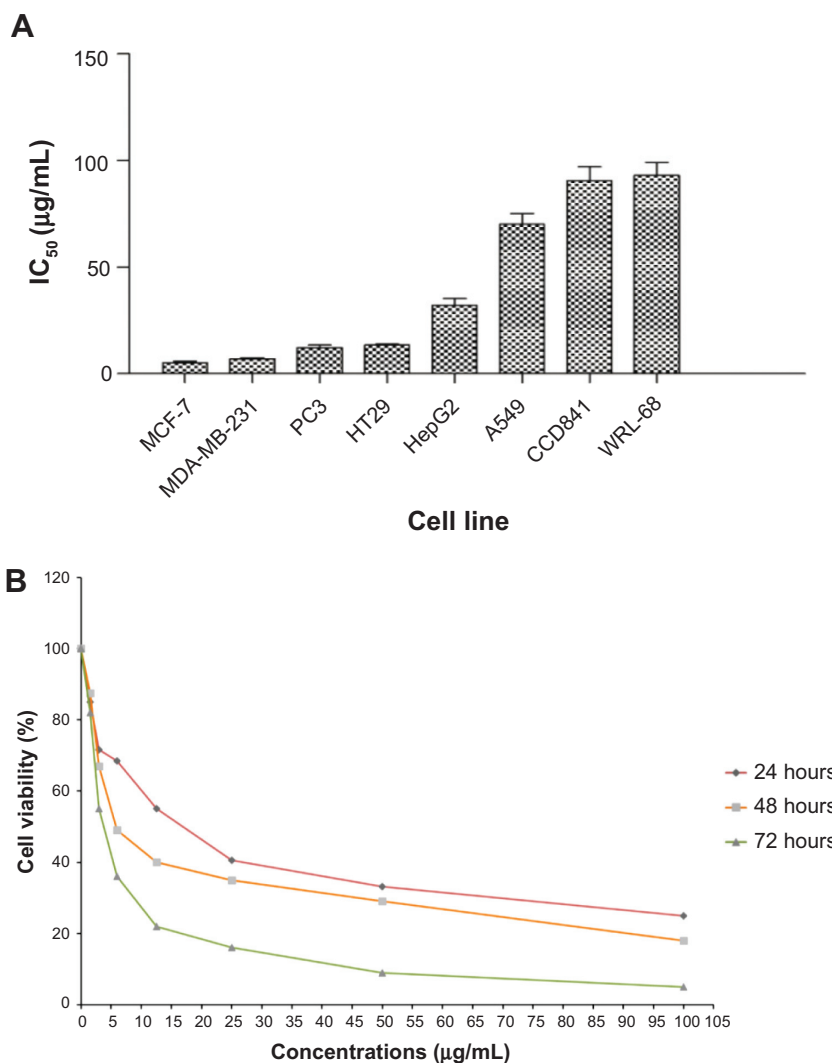

Figure 1 Suppressive effect of FALHE against cancer and normal cells.
Notes: (**A**) IC_{50} concentration of FALHE on eight different cell lines after 48 hours of treatment. (**B**) FALHE suppressed MCF-7 cell proliferation in a concentration- and time-dependent manner. *$P<0.05$.
Abbreviations: IC_{50}, half maximal inhibitory concentration; FALHE, *Ferulago angulata* leaves hexane extract.
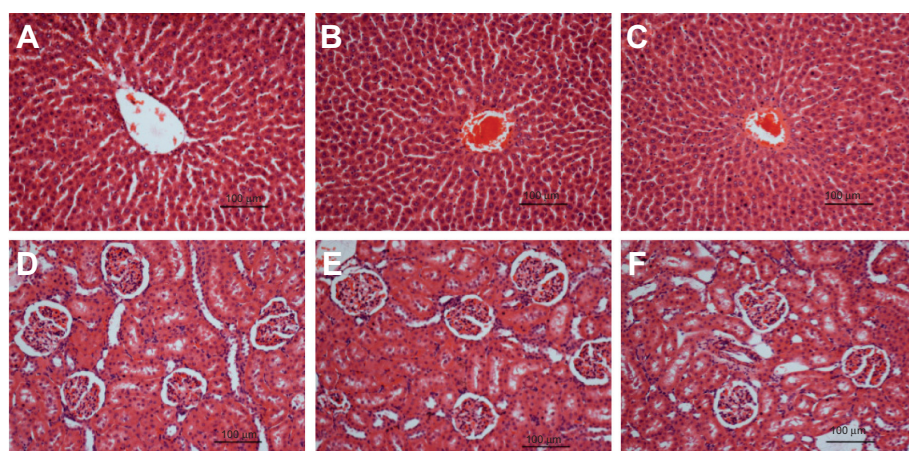
Figure 2 Histological sections of liver and kidney.
Notes: Histological (hematoxylin and eosin stain, 20×) of liver (**A–C**) and kidney (**D–F**) did not show any abnormality after treatment with (**B** and **E**) 2 g/kg and 5 g/kg (**C** and **F**) of FALHE, compared to the vehicle 10% Tween-20 (**A** and **D**).
Abbreviation: FALHE, *Ferulago angulata* leaves hexane extract.

and KG-1A (human acute myelocytic leukemia) cell lines showed relatively high IC_{50} values of 96.81, 158.68, and 128.47 µg/mL, respectively.[26]

Safety of FALHE

The extensive traditional use of plant remedies by natives for a long period of time without any report of toxicity or adverse side effects can generally provide some evidence for the safety of the respective plant.[32] However, previous studies showed that some chemical constituents or secondary metabolites present in traditional medicines have toxic or even carcinogenic effects on human body.[32–34] Therefore, investigation on the safety of plants prior to performing any experiment on their biological activity is highly recommended to avoid any undesirable adverse side effects.

The acute toxicity study of FALHE demonstrated the safety of this extract, since during the 14 days period all the rats remained alive and did not show any sign of toxicity even at a high dose of 5 g/kg. In addition, histological, hematological, and serum biochemical analysis did not show any sign of hepatic or renal toxicity in the treatment groups (Figure 2; Table S1).

Chemical analysis of FALHE

The chemical composition of FALHE was characterized using GC-MS-TOF analysis (Figure 3). The chromatogram showed two monoterpenoid phenols as major compounds, ie, thymol (3, $C_{10}H_{14}O$) and carvacrol (4, $C_{10}H_{14}O$) (Table 1). Previous studies showed that these two phenolic compounds have promising anticancer effects against cancer cell lines. Thymol was found to induce apoptosis in HL-60 cells through both caspase-dependent and caspase-independent pathways.[35] The marked antiproliferative effect of carvacrol and its mechanism of action toward different cancer cells,

Table 1 GC-MS-TOF analysis showed eleven detected compounds in FALHE

Peak	Name of compound	Retention time (seconds)	Mass (g/mol)
1	Methanesulfonyl acetic acid	284.35	138
2	Heptane, 2-methyl	542.5	114
3	Thymol	714.1	150
4	Carvacrol	714.8	150
5	2(4)-benzofuranone, 5,6,7,7a-tetrahydro-4,4,7a-trimethyl	1,533.85	180
6	2-pentanone,4-hydroxy-4-methyl	3,233.5	116
7	4a-methyl-1-methylene-1,2,3,4,4a,9,10,10a-octahydrophenanthrene	3,260.6	197
8	1-ethoxy-7-phenylvinylidene-bicyclo heptane	3,335.7	240
9	6H-dibenzo-pyran	3,474.9	181
10	Aromadendrene epoxide	3,550.55	205
11	9-octadecenamide	3,625.3	281

Abbreviations: GC, gas chromatography; MS, mass spectrometry; TOF, time of flight analysis; FALHE, *Ferulago angulata* leaves hexane extract.
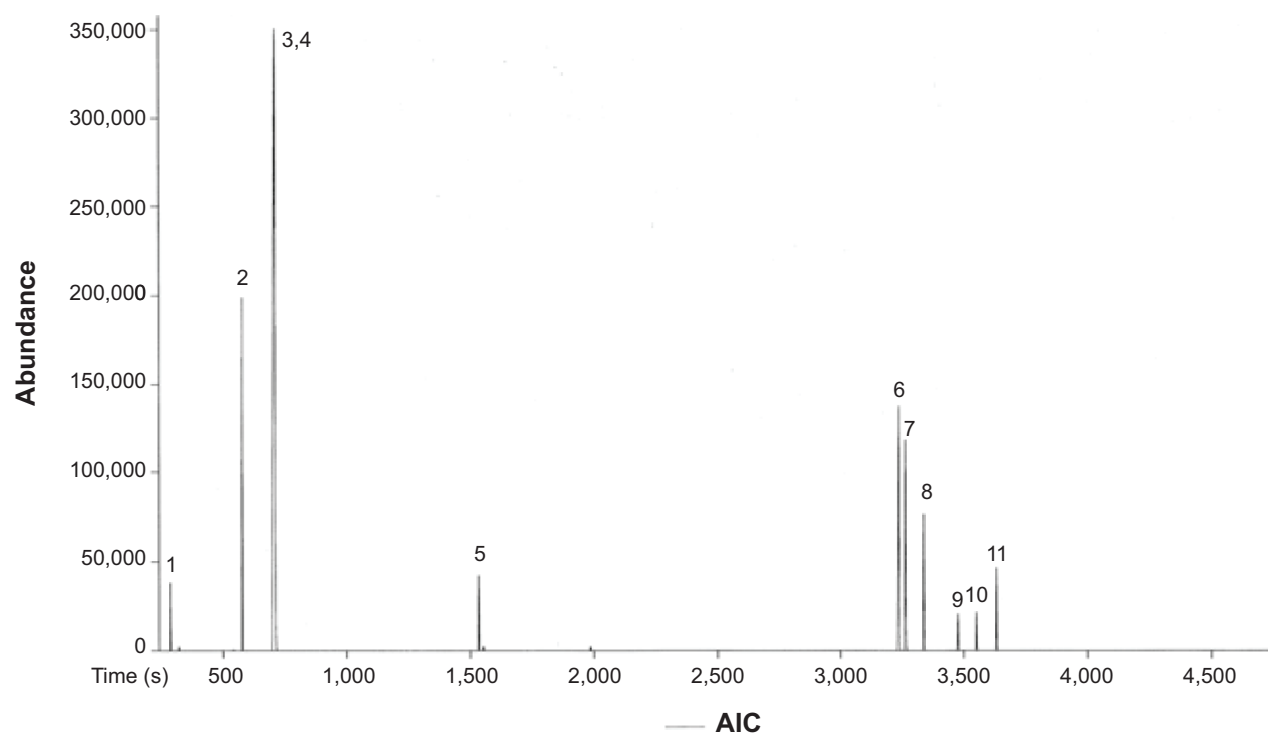
Figure 3 Chemical constituents of FALHE determined by a gas chromatogram analysis.
Note: 3 (Thymol) and 4 (Carvacrol) are the major compounds based on their intensity.
Abbreviations: FALHE, *Ferulago angulata* leaves hexane extract; AIC, analytical ion chromatogram.
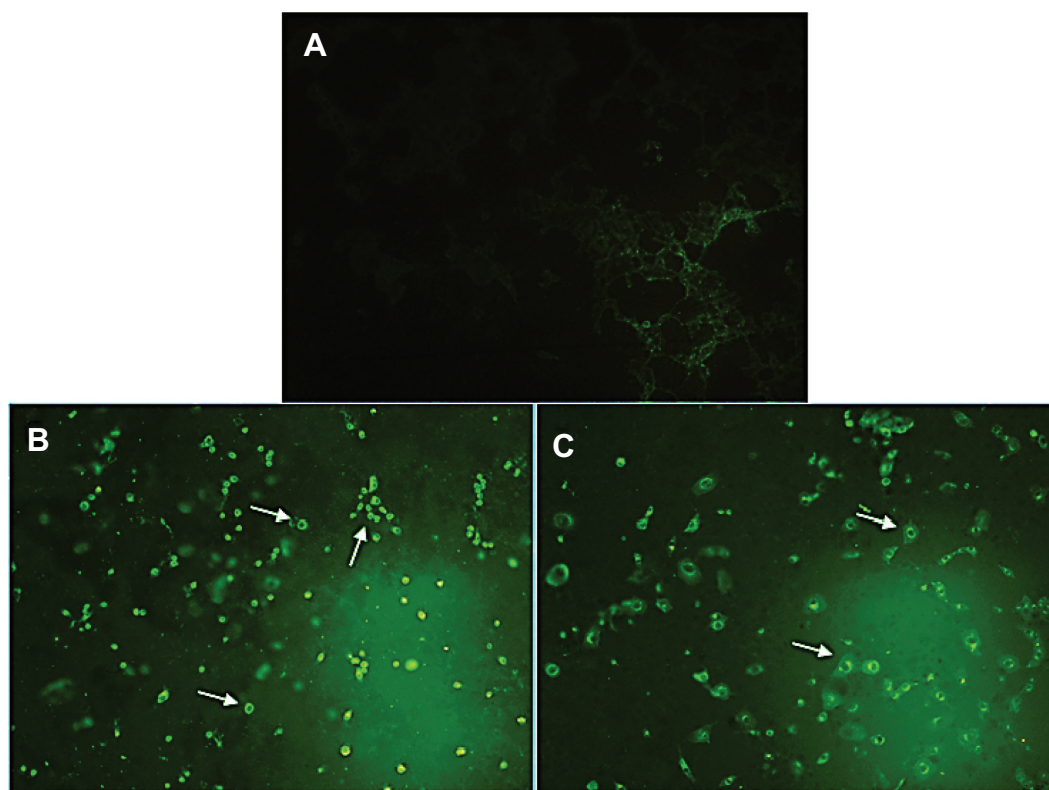

Figure 4 Microscopic evaluation of the PS externalization.
Notes: (**A**) Untreated cells (control) did not show any sign of PS translocation as an early marker for apoptosis. After 48 hours of treatment with IC$_{50}$ concentration of FALHE, annexin-V-FITC binding to PS residues shown in the light green stain demonstrated the externalization of PS. The treated cells were shown with (**B**) 20× and (**C**) 40× magnifications. The white arrows show the PS externalization in treated cells.
Abbreviations: PS, phosphatidylserine; IC$_{50}$, half maximal inhibitory concentration; FALHE, *Ferulago angulata* leaves hexane extract; FITC, fluorescein isothiocyanate.

including MDA-MB-231,[36] HepG-2,[37] and A549[38] cells, has previously been investigated. The suppressive effects of these two phenolic compounds on cancer cells are closely correlated with the IC_{50} value of FALHE toward different cancer cells. However, a study with a bioassay-guided approach on FALHE is further required to certainly determine the major

bioactive compounds responsible for the observed cytotoxic effects, which is ongoing in our laboratory.

Externalization of PS induced by FALHE

Apoptotic properties of cancer cells are the critical key to most of the approaches applied in radiation and chemotherapy.
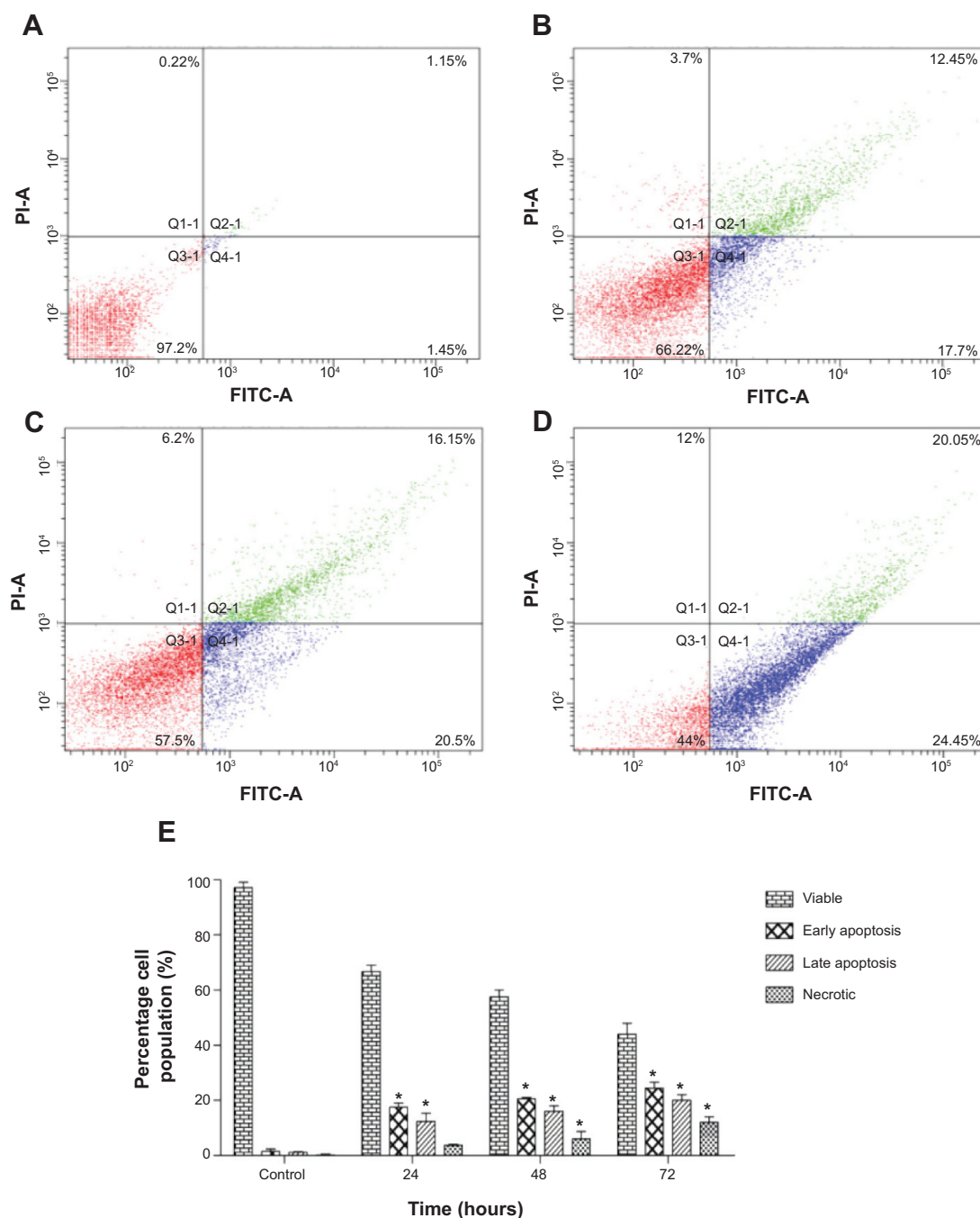
Figure 5 Flow cytometric analysis of apoptosis in MCF7 cells.
Notes: (**A**) Shows the untreated MCF-7 cells (control) after 72 hours. After treatment with IC_{50} concentration of FALHE for (**B**) 24, (**C**) 48 and (**D**) 72 hours, flow cytometry analysis was carried out on MCF7 treated and untreated cells. Meanwhile, (**E**) representative bar chart showed a significant elevation in the number of apoptotic and necrotic cells after 72 hours. *$P<0.05$.
Abbreviation: FALHE, *Ferulago angulata* leaves hexane extract.

Thus, it has considerable therapeutic implications.[39] Apoptosis is characterized by various biochemical changes in cells, mainly nuclear condensation, DNA fragmentation, PS externalization, MMP changes, membrane blebbing, and regulations in caspases' enzymes. These changes are considered as the biomarkers of apoptosis.[40]

PCD (apoptosis) has two distinct phases, namely, early and late apoptosis. A simple and noninvasive assay of annexin-V-FITC is designed for early detection of apoptosis. PS, which is normally located on the inner surface of the plasma membrane, translocates to the outer surface of the plasma membrane after an induction of apoptosis, apparently through an active mechanism.[41] Annexin-V-FITC is

a probe with a high affinity for PS, which has provided an easy method for the detection of apoptosis, since PS exposure is a widespread event during apoptosis, which occurs prior to membrane leakage and DNA-associated changes.[42] As shown in Figure 4, the treatment of MCF-7 cells with the IC$_{50}$ concentration of FALHE-induced translocation of PS to the outer membrane after 48 hours, while there was no sign of translocation in the control cells.

To confirm the microscopic detection of PS externalization, we carried out the flow cytometric analysis using annexin-V-FITC and PI double staining. Treatment with FALHE for 24 hours significantly elevated the number of early (annexin-V positive; PI negative) and late (annexin positive;
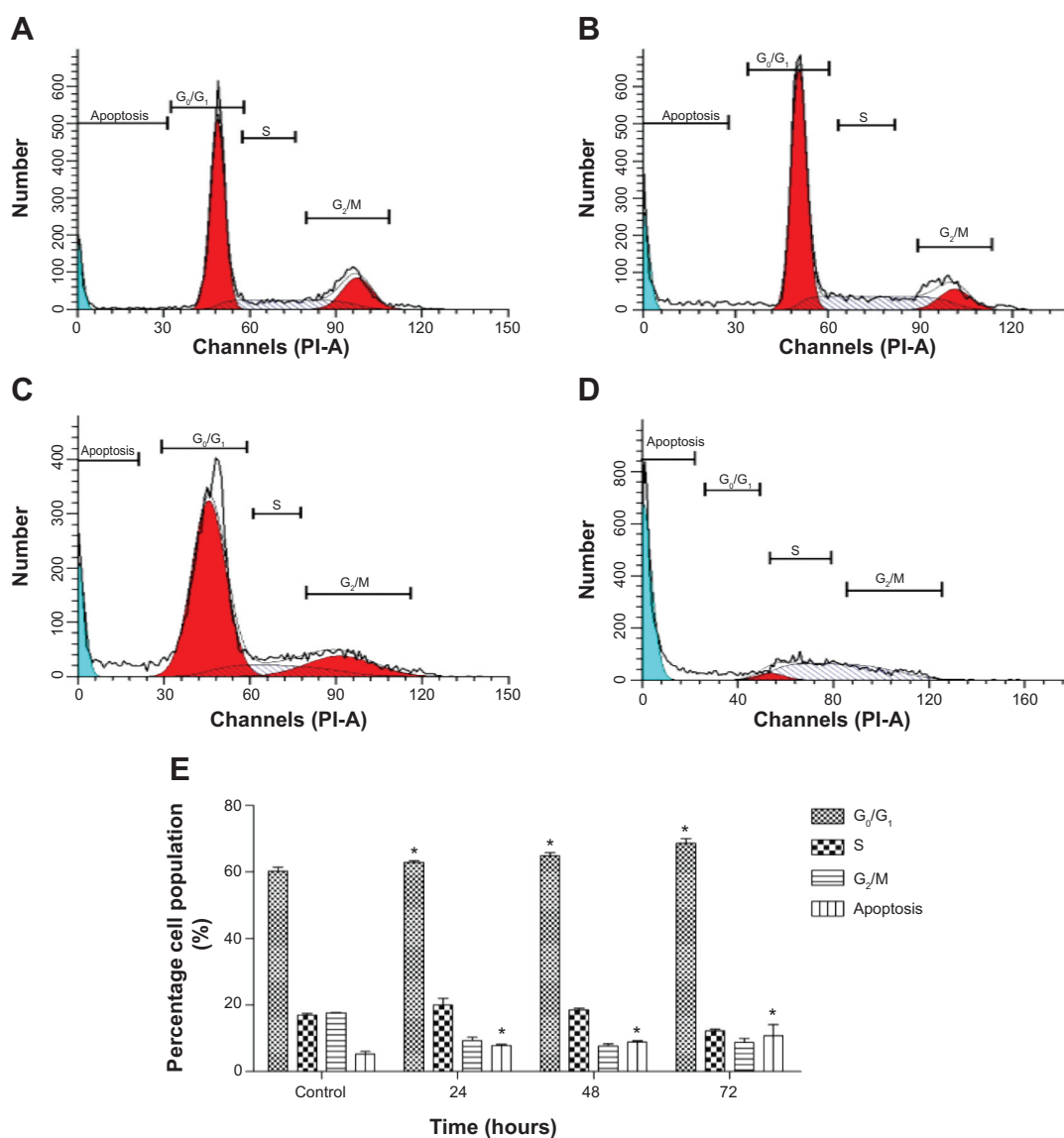

Figure 6 Effect of FALHE on cell cycle distribution of MCF-7 cells.
Notes: (**A**) Shows the untreated MCF-7 cells (control) after 72 hours. After treatment with IC$_{50}$ concentration of FALHE for (**B**) 24, (**C**) 48 and (**D**) 72 hours, flow cytometry analysis was carried out on MCF7 treated and untreated cells. (**E**) The quantitative analysis shows the cell cycle arrest at G$_0$/G$_1$ phase. (*$P < 0.05$).
Abbreviations: FALHE, *Ferulago angulata* leaves hexane extract; IC$_{50}$, half maximal inhibitory concentration; G, gap; S, synthesis; M, mitosis.

PI positive) apoptotic cells to 17.7% and 12.45%, respectively (Figure 5B). These numbers reached to 20.5% and 16.15% after 48 hours of treatment, respectively (Figure 5C). Meanwhile, the number of necrotic cells also significantly increased after 48 hours and 72 hours (Figure 5D), which was expected since due to the long incubation time with FALHE and its cytotoxic effects, some cells showed necrotic characterizations.[43] The result of flow cytometric analysis confirmed the induction of apoptosis by FALHE in a time-dependent manner (Figure 5E).

Cell cycle arrest at G_1 phase induced by FALHE

Previous studies[44,45] have reported that the regulation of cell death and cell proliferation shares prevalent proteins and molecules in multicellular organisms. Indeed, cell cycle regulation and apoptosis are regulated by several mutual genes.[44] A direct correlation between apoptosis and cell cycle shows that apoptosis and mitosis have very close morphological characteristics. During either of the processes, after the cells detach, they become rounded, condense their chromatin, and display membrane blebbing.[45] In spite of some shared features, there are critical differences between mitosis and apoptosis.[46] For example, cell membrane proteins are cross-linked during apoptosis, resulting in the rigidity of the membrane, and apoptotic cells are normally phagocytized by macrophages or adjacent cells. In contrast, during mitosis, the segregation of DNA and the division of the cell by cytokinesis leading to two healthy and viable daughter cells, are observed.[47] To analyze the respective connection, we investigated the cell cycle progression in MCF-7 cells upon treatment with FALHE in a time-dependent pattern for 24, 48, and 72 hours. This experiment was carried out to determine the effect of FALHE

on the DNA content of MCF-7 cells by cell cycle phase distribution (gap $[G]_0/G_1$, synthesis [S], and G_2/mitosis [M]) (Figure 6). The results demonstrated that the FALHE significantly arrested the cell cycle progression at the G_1 phase in a time-dependent manner. The number of MCF-7 cells at this phase increased from 58.93% (untreated control) to 67.31% (72 hours). Meanwhile, the number of cells in the S and G_2/M phases reduced after 72 hours of treatment compared to the control. Furthermore, the significant and time-dependent elevation in the cell population at sub-G_1 phase presenting the hypodiploid DNA in MCF-7 cells elicited the number of cells undergoing apoptosis.

Caspase-8 and caspase-9 activation induced by FALHE

The caspase cascade signaling system is a critical factor in the process of apoptosis, which is precisely controlled by a variety of proapoptotic and antiapoptotic molecules.[48] After treatment of MCF-7 cells with IC_{50} concentration of FALHE for 3, 6, 12, 24, 48, and 72 hours, caspase-8 and caspase-9 enzyme activity was evaluated. The activity of caspase-8 significantly increased at 72 hours, while caspase-9 activity significantly rose at 12, 24, 48, and 72 hours of treatment (Figure 7). The apoptosis-inducing potential of FALHE through the mitochondrial pathway was confirmed by the activation of caspase-9 after 12 hours. Furthermore, the elevated activity of caspase-8 after treatment with FALHE has thrown light on the possible contribution of extrinsic pathway to the induction of apoptosis by FALHE at the late stage of treatment. Involvement of more than a single apoptotic pathway in the induction of PCD by anticancer compounds is well-established, especially by plant-derived natural agents, such as curcumin.[49,50] In this study, untreated cells
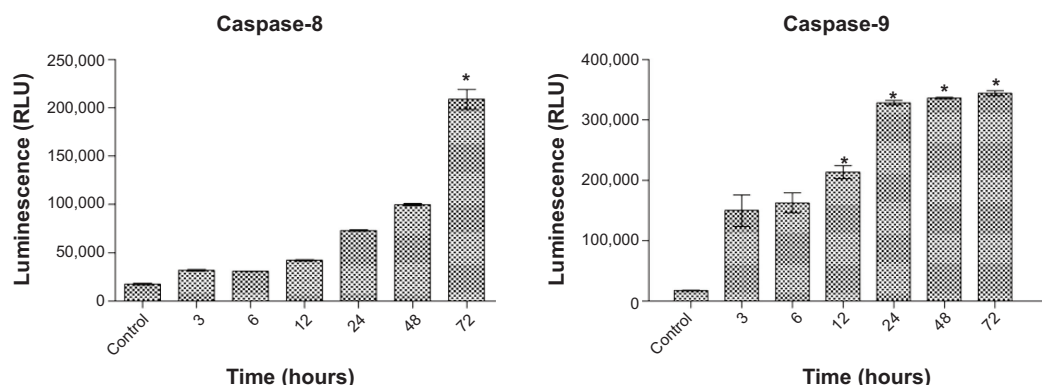

Figure 7 Luminescence assay.
Notes: The luminescence assay revealed an activation of caspase-9 after 12 hours and caspase-8 after 72 hours of treatment with FALHE. *P<0.05.
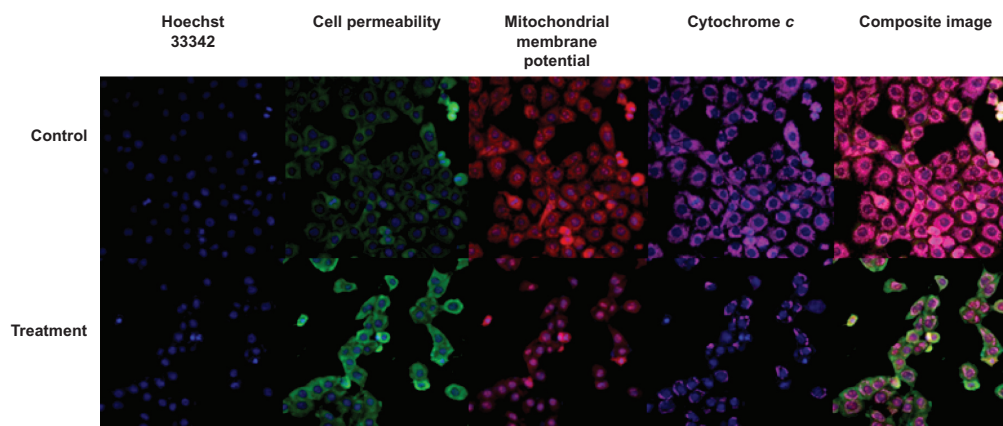**Abbreviations:** FALHE, *Ferulago angulata* leaves hexane extract; RLU, Relative luminescence unit.

Figure 8 Images of MCF-7 cells.
Notes: These images of MCF-7 cells (×20) were treated with FALHE at IC_{50} concentration, stained with different specific dyes, detecting total nuclear intensity, MMP, cytochrome *c* release, and cell membrane permeability. The images from each row were captured from the specific field of treated sample.
Abbreviations: FALHE, *Ferulago angulata* leaves hexane extract; IC_{50}, half maximal inhibitory concentration; MMP, mitochondrial membrane potential.

did not show any increase in the activity of caspase-8 and caspase-9; however, activity was significantly and time dependently elevated after treatment with FALHE. The role of caspase-9 has previously been determined to be a step prior to the activation cascade of the mitochondrial pathway that results in apoptosis.[51] Caspase-9 activation is heavily regulated by apoptosome, which converts procaspase-9 to caspase-9 by enzymatic cleavage.[15]

Multiparameter cytotoxicity analysis

To determine the possible mechanism of action for the induced apoptosis by FALHE, we investigated critical biochemical and morphological changes in MCF-7 cells, in specific nuclear condensation, and in mitochondrial-initiated events. Hoechst 33342 staining demonstrated that numerous cells treated with FALHE displayed nuclear condensation shown with blue fluorescent intensity (Figure 8).
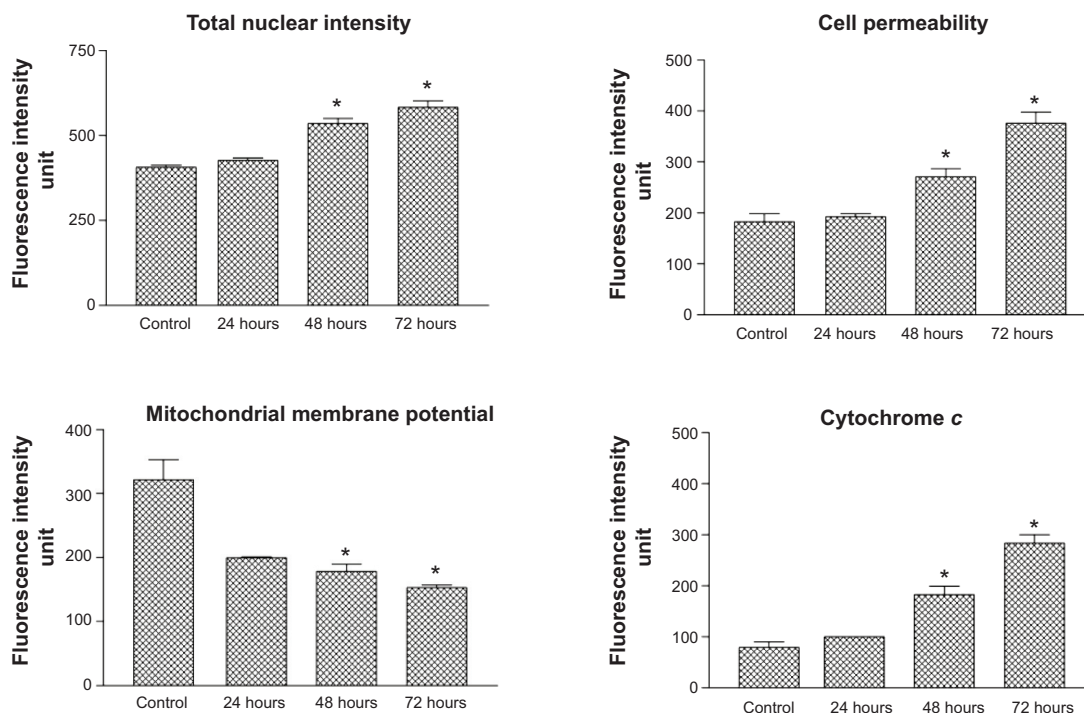

Figure 9 Quantitative analysis of multiparameter cytotoxicity assay revealed changes in total nuclear intensity, cell membrane permeability, MMP, and cytochrome *c* release.
Notes: Following treatment with FALHE for 48 hours, significant elevation in total nuclear intensity, cell membrane permeability, cytochrome *c* release associated with reduction in MMP were detected. (*$P < 0.05$).
Abbreviations: MMP, mitochondrial membrane potential; FALHE, *Ferulago angulata* leaves hexane extract.
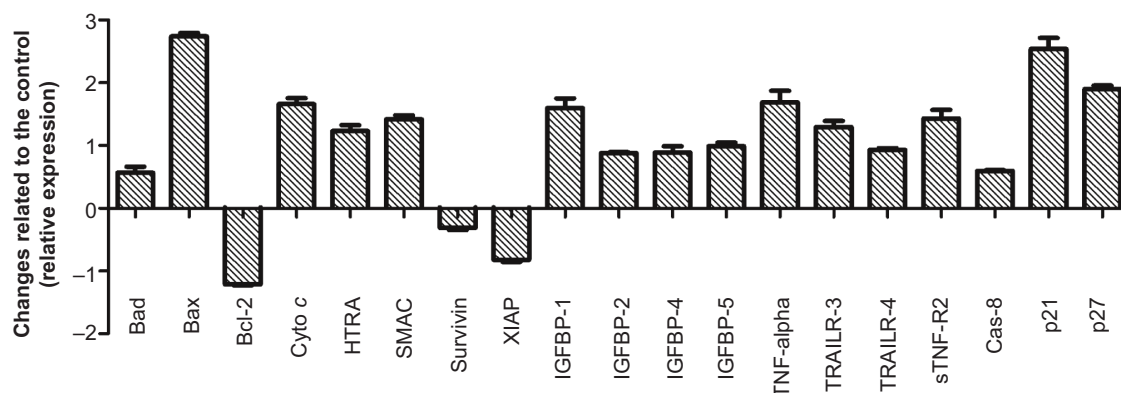
Figure 10 Graph demonstrates the difference between treated and untreated cells.
Notes: Human apoptosis proteome profiler array in MCF-7 cells treated with FALHE at IC$_{50}$ concentration for 48 hours. *$P<0.05$.
Abbreviations: SMAC, second mitochondria-derived activator of caspases; XIAP, X-linked inhibitor of apoptosis protein; IGFBP, insulin-like growth factor binding proteins; TNF, tumor necrosis factor; TRAILR, TNF-related apoptosis-inducing ligand; IC$_{50}$, half maximal inhibitory concentration.

Nuclear intensity (which directly corresponds to apoptotic chromatin changes), cell membrane permeability, MMP, and cytochrome *c* release were quantified (Figure 9). Nuclear intensity significantly increased after 48 hours of treatment with FALHE. A concurrent elevation in the cell membrane permeability shown with green fluorescent intensity was also exhibited for the same period (Figure 8). MMP was significantly decreased in the MCF-7 cells treated with FALHE, as shown by a conspicuous attenuation in the red fluorescent intensity (Figure 8).

Furthermore, FALHE triggered a significant translocation of cytochrome *c* from mitochondria into cytosol. At 48 hours, FALHE triggered approximately threefold cytochrome *c* release represented by cyan fluorescent intensity in Figure 8.

Apoptosis proteome profiler analysis

To further examine the detailed pathways responsible for induced apoptosis by FALHE toward MCF-7 cells, screening of critical proteins that are involved in various pathways of apoptosis was carried out. As shown in Figure 10, critical proteins involved in the intrinsic pathway of apoptosis, including Bad, Bax, cytochrome *c*, second mitochondria-derived activator of caspases (SMAC)/DIABLO, and serine protease HtrA2/Omi were significantly overexpressed after 48 hours of treatment, while the expression of antiapoptotic proteins of Bcl-2, survivin, X-linked inhibitor of apoptosis protein (XIAP) were downregulated. Additionally, p21 and p27, which are cell proliferation suppressor proteins, were upregulated. Different insulin-like growth factor binding proteins (IGFBPs) were also upregulated while treatments. Specific ligands of the tumor necrosis factor (TNF)-α involved in the extrinsic pathway and death receptors, such as

soluble TNF receptor (R) 2, TNF-related apoptosis-inducing ligand (TRAIL)R-3, and TRAILR-4 were slightly induced by treatment with FALHE.

The induced apoptosis by FALHE was associated with significant changes in the expression level of proteins from Bcl-2 family. We found out that the expression of the antiapoptotic protein of Bcl-2 was significantly reduced, while proapoptotic proteins of the Bcl-2 family, including Bax and Bad, were significantly expressed after treatment with FALHE. Changes in the expression of the Bcl-2 family proteins led to the overexpression of cytochrome *c*, which resulted in the translocation of cytochrome *c* from the mitochondria to the cytosol as proved by the multiparameter cytotoxicity assay.[52] Besides cytochrome *c*, there are other proteins, such as SMAC/DIABLO and the serine protease HtrA2/Omi, that are released through the mitochondrial permeability transition pores provided by Bax protein in the inner mitochondrial membrane.[53]

Cytochrome *c* release has a critical role in the activation of the intrinsic pathway of apoptosis as an important factor in the formation of the apoptosome, while SMAC/DIABLO and HtrA2/Omi suppress the activity of inhibitors of apoptosis proteins (IAPs), such as survivin and XIAP, whose expression was significantly reduced in our experiment.[54] IGFBPs have been proved to significantly suppress the proliferation of different cell types. Previous studies have shown that IGFBPs are involved in the induction of apoptosis in MCF-7 cells via a death receptor-mediated pathway.[55] The activation of apoptosis by a death receptor-mediated pathway was also suggested by the expression of TNF-α as the activator ligand for the death receptors, including TNFR1 and TNFR2, which are involved in the extrinsic pathway.[56] In addition, the activation of caspase-8 after
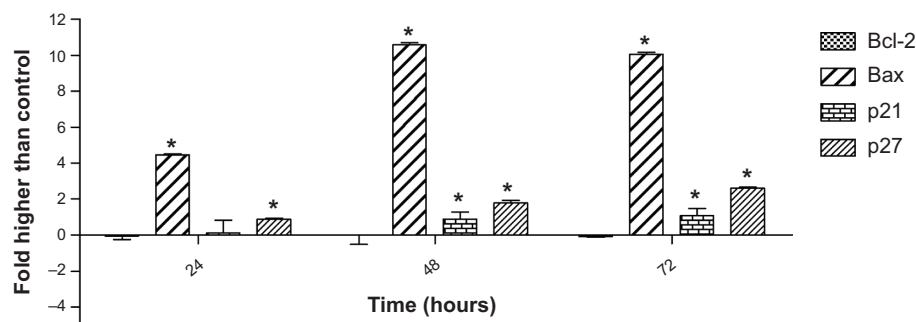
Figure 11 Quantitative analysis of gene expression.
Notes: Quantitative analysis of gene expression in MCF-7 cells after 72 hours of treatment with FAHLE showed a significant elevation in the expression of Bax, p21, and p27 genes, compared to the control. Meanwhile, gene expression of Bcl-2 did not elicit significant changes. *$P<0.05$.
Abbreviation: FAHLE, *Ferulago angulata* leaves hexane extract.

72 hours of treatment with FALHE compared to the activation of caspase-9 after 12 hours of treatment, as shown in the luminescence analysis, suggests an activation of the intrinsic pathway followed by an activation of the extrinsic pathway at the late stage of treatment. Additionally, the cell cycle has been shown to be involved in the suppression of cyclin-dependent kinases, which are responsible for the G_1-to-S transition.[57]

FALHE upregulated the gene expression of Bax, p21, and p27

Since the protein array analysis showed the most significant changes in the expression of the Bcl-2, Bax, p21, and p27 proteins, we investigated the expression of these proteins at the gene level, using the quantitative polymerase chain reaction analysis. The result showed a significant elevation in the gene expression of Bax, p21, and p27, which supported our findings
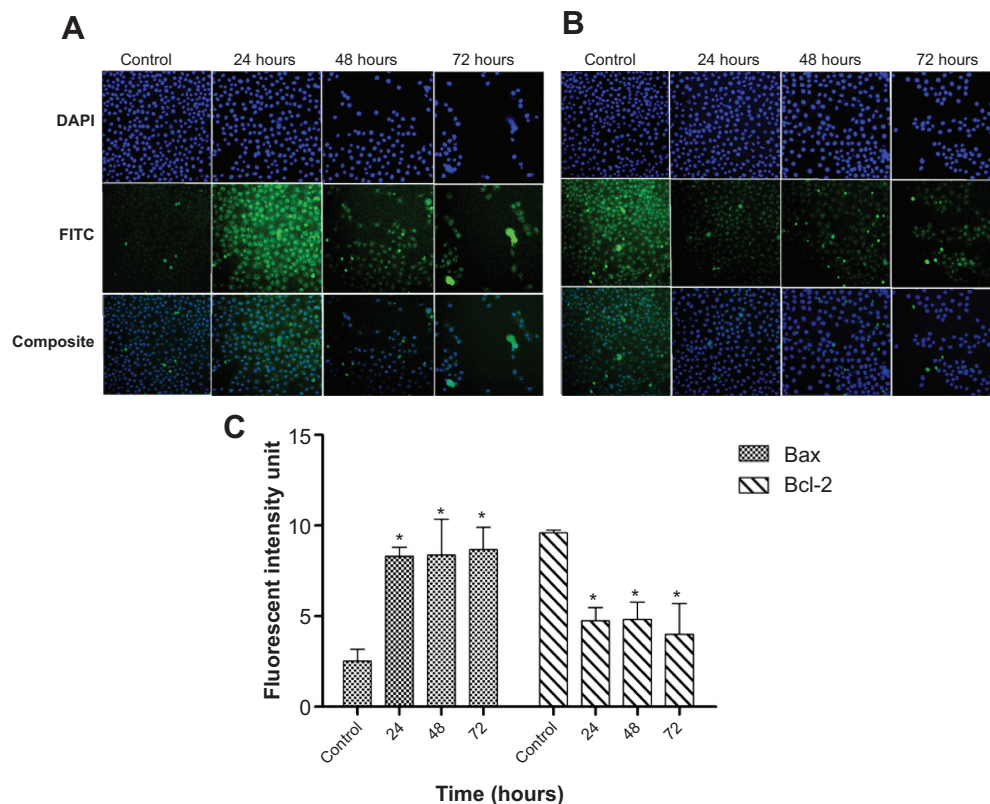

Figure 12 Immunofluorescence analysis.
Notes: An immunofluorescence analysis of (**A**) Bax and (**B**) Bcl-2 in MCF-7 cells depicted a marked elevation in the fluorescent intensity of Bax and reduction in the fluorescent intensity of Bcl-2 antibodies conjugated to FITC, in a time-dependent manner. (**C**) Quantitative analysis of Bax and Bcl-2 expression in MCF-7 cells showed a time dependent increase in the Bax expression and decrease in the Bcl-2 expression at the protein level. *$P<0.05$.
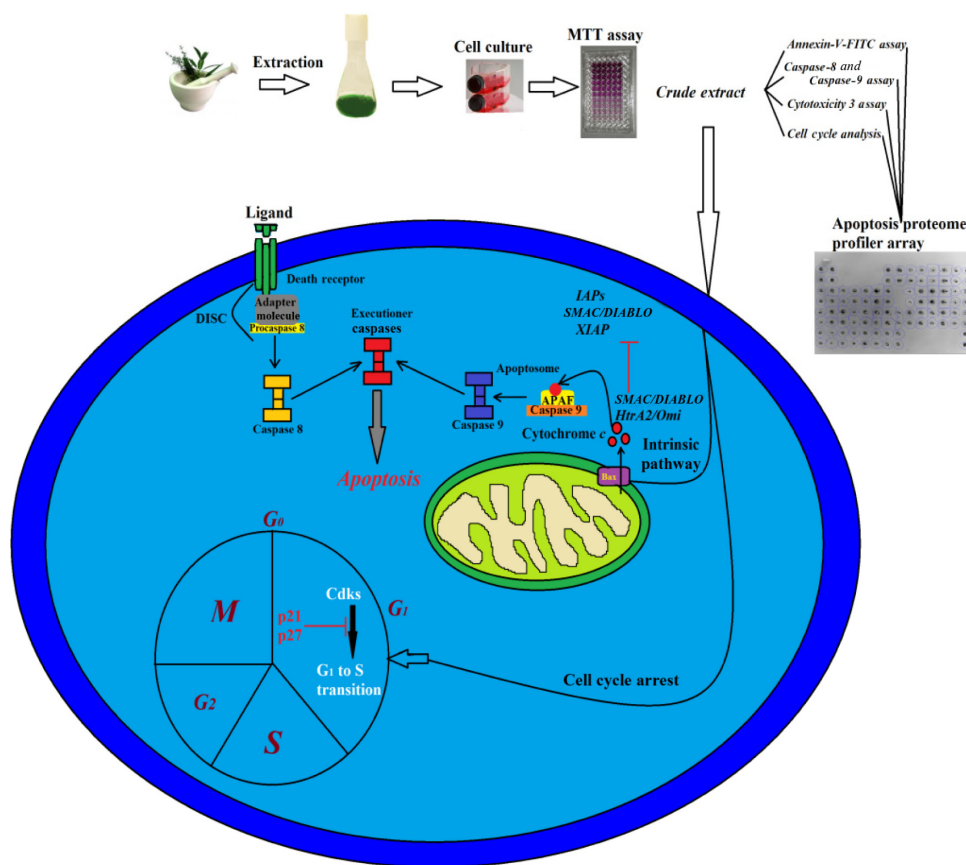**Abbreviation:** FITC, fluorescein isothiocyanate.

Figure 13 Illustration of the possible molecular pathway for the induced apoptosis triggered by FALHE.
Abbreviations: FALHE, *Ferulago angulata* leaves hexane extract; IAP, inhibitors of apoptosis proteins; SMAC, second mitochondria-derived activator of caspases; XIAP, X-linked inhibitor of apoptosis protein; M, mitosis; G, gap; S, synthesis; CDK, cyclin-dependent kinases; FITC, fluorescein isothiocyanate.

from the protein array analysis. However, Bcl-2 gene expression did not significantly change during 72 hours of treatment (Figure 11). These results suggest that FALHE treatment induces cell cycle arrest at the G_1 phase via overexpression of p21 and p27 at the gene level. Recent studies on the p21 and p27 proteins have determined the critical role of these cell-cycle inhibitors on cell division and, subsequenltly, on cancer therapy approaches, since various cancer cells contain mutations in members of the proteins that regulate cyclin-dependent kinase activity.[58,59] Therefore, apoptotsis-inducing agents with the ability to upregulate p21 and p27 proteins at the gene and protein level can be identified as promising anticancer agents.

FALHE upregulated the protein expression of Bax and downregulated the protein expression of Bcl-2

Due to the important role of Bcl-2 and Bax proteins in the mitochondrial-dependent apoptosis, expression of these proteins was investigated using immunofluorescence analysis. DAPI dye was used to stain the nucleus of the MCF-7 cells and in determining the number of cells. As shown in Figure 12,

the number of MCF-7 cells decreased in a time-dependent manner in the treatment group as compared to the control group. The fluorescent intensity of the Bax-conjugated antibody was markedly increased after increasing the time of treatment with FAHLE (Figure 12A). In contrast, the fluorescent intensity of Bcl-2 was conspicuously decreased in the same time period (Figure 12B). Quantitative analysis of the result showed a significant upregulation of Bax associated with significant downregulation of Bcl-2 after 24, 48, and 72 hours of treatment (Figure 12C). The perturbation in the protein expression of Bcl-2 compared to its unchanged gene expression after 72 hours of treatment suggested that in spite of FALHE treatment, the Bcl-2 gene was still expressed and its activity was only significantly suppressed at the protein level. However, Bax expression was upregulated both at the gene and protein level.

Conclusion

In conclusion, the plant *F. angulata* has been found to have the potential of inducing mitochondrial-mediated apoptosis in MCF-7 cells through the activation of caspase enzymes.

Furthermore, the active role of mitochondria in the induction of apoptosis was confirmed by the release of cytochrome *c* and reduction in MMP. The cell cycle arrest in G_1 phase was proved to be one of the possible mechanisms for suppressing cell proliferation, which suggests to be induced by the upregulation of p21 and p27 proteins. The suggested molecular pathway for the induced apoptosis is summarized in Figure 13. Our result demonstrated that *F. angulata* is a promising plant for cancer therapy. However, further in vitro and in vivo studies on the active compounds of this plant are still required.

Acknowledgments

Disclosure

The authors report no conflicts of interest in this work.

References

1. David AR, Zimmerman MR. Cancer: an old disease, a new disease or something in between? *Nat Rev Cancer.* 2007;10(10):728–733.
2. Guo SP, Wu SG, Zhou J, et al. Transdermal fentanyl for pain due to chemoradiotherapy-induced oral mucositis in nasopharyngeal cancer patients: evaluating efficacy, safety, and improvement in quality of life. *Drug Des Devel Ther.* 2014;8:497–503.
3. Rabik CA, Dolan ME. Molecular mechanisms of resistance and toxicity associated with platinating agents. *Cancer Treat Rev.* 2007;33(1):9–23.
4. Meyer zu Schwabedissen HE, Kroemer HK. In vitro and in vivo evidence for the importance of breast cancer resistance protein transporters (BCRP/MXR/ABCP/ABCG2). *Handb Exp Pharmacol.* 2011;(201):325–371.
5. Perez EA. Impact, mechanisms, and novel chemotherapy strategies for overcoming resistance to anthracyclines and taxanes in metastatic breast cancer. *Breast Cancer Res Tr.* 2009;114(2):195–201.
6. Hajrezaie M, Paydar M, Moghadamtousi SZ, et al. A Schiff base-derived copper (II) complex is a potent inducer of apoptosis in colon cancer cells by activating the intrinsic pathway. *Scientific World Journal.* 2014;2014:540463.
7. Moghadamtousi SZ, Goh BH, Chan CK, Shabab T, Kadir HA. Biological activities and phytochemicals of Swietenia macrophylla King. *Molecules.* 2013;18(9):10465–10483.
8. Lantto TA, Dorman HJ, Shikov AN, et al. Chemical composition, antioxidative activity and cell viability effects of a Siberian pine (*Pinus sibirica* Du Tour) extract. *Food Chem.* 2009;112(4):936–943.
9. Mishra BB, Tiwari VK. Natural products: an evolving role in future drug discovery. *Eur J Med Chem.* 2011;46(10):4769–4807.
10. Shoeb M. Anticancer agents from medicinal plants. *Bangladesh Journal of Pharmacology.* 2006;1(2):35–41.
11. Newman DJ, Cragg GM. Natural products as sources of new drugs over the last 25 years. *J Nat Prod.* 2007;70(3):461–477.
12. Newman DJ, Cragg GM. Natural products as sources of new drugs over the 30 years from 1981 to 2010. *J Nat Prod.* 2012;75(3):311–335.
13. Shimizu S, Yoshida T, Tsujioka M, Arakawa S. Autophagic cell death and cancer. *Int J Mol Sci.* 2014;15(2):3145–3153.
14. Díaz LF, Chiong M, Quest AF, Lavandero S, Stutzin A. Mechanisms of cell death: molecular insights and therapeutic perspectives. *Cell Death Differ.* 2005;12(11):1449–1456.
15. Elmore S. Apoptosis: a review of programmed cell death. *Toxicol Pathol.* 2007;35(4):495–516.
16. Indran IR, Tufo G, Pervaiz S, Brenner C. Recent advances in apoptosis, mitochondria and drug resistance in cancer cells. *Biochim Biophys Acta.* 2011;1807(6):735–745.
17. Martinou JC, Youle RJ. Mitochondria in apoptosis: Bcl-2 family members and mitochondrial dynamics. *Dev Cell.* 2011;21(1):92–101.
18. Petit PX, Lecoeur H, Zorn E, Dauguet C, Mignotte B, Gougeon ML. Alterations in mitochondrial structure and function are early events of dexamethasone-induced thymocyte apoptosis. *J Cell Biol.* 1995;130(1):157–167.
19. Tan S, Sagara Y, Liu Y, Maher P, Schubert D. The regulation of reactive oxygen species production during programmed cell death. *J Cell Biol.* 1998;141(6):1423–1432.
20. Ka H, Park HJ, Jung HJ, et al. Cinnamaldehyde induces apoptosis by ROS-mediated mitochondrial permeability transition in human promyelocytic leukemia HL-60 cells. *Cancer Lett.* 2003;196(2):143–152.
21. Sodeifian G, Ansari K. Optimization of Ferulago Angulata oil extraction with supercritical carbon dioxide. *J Supercrit Fluids.* 2011;57(1):38–43.
22. Sodeifian G, Ansari K, Bamoniri A, Mirjalili BF. Study of chemical composition of the essential oil of Ferulago angulata (Schelcht) Boiss. from iran using supercritical fluid extraction and nano scale injection. *Digest Journal of Nanomaterials and Biostructures.* 2011;6(1):161–168.
23. Mirzaaghaei S, Akrami H, Mansouri K. Ferulago angulata flower and leaf extracts inhibit angiogenesis in vitro through reducing VEGF-A and VEGFR-2 genes expression. *Arch Iran Med.* 2014;17(4):278–285.
24. Taran M, Ghasempour HR, Shirinpour E. Antimicrobial activity of essential oils of Ferulago angulata subsp. carduchorum. *Jundishapur Journal of Microbiology.* 2011;3(1):10–14.
25. Amirghofran Z, Bahmani M, Azadmehr A, Javidnia K. Anticancer effects of various Iranian native medicinal plants on human tumor cell lines. *Neoplasma.* 2006;53(5):428–433.
26. Shahneh FZ, Valiyari S, Azadmehr A, Hajiaghaee R, Bandehagh A, Baradaran B. Cytotoxic activities of *Ferulago angulata* extract on human leukemia and lymphoma cells by induction of apoptosis. *Journal of Medicinal Plants Research.* 2013;7(11):677–682.
27. Daferera DJ, Ziogas BN, Polissiou MG. GC-MS analysis of essential oils from some Greek aromatic plants and their fungitoxicity on Penicillium digitatum. *J Agric Food Chem.* 2000;48(6):2576–2581.
28. Vermes I, Haanen C, Steffens-Nakken H, Reutellingsperger C. A novel assay for apoptosis. Flow cytometric detection of phosphatidylserine expression on early apoptotic cells using fluorescein labelled Annexin V. *J Immunol Methods.* 1995;184(1):39–51.
29. Sulaiman Rahman H. A phenylbutenoid dimer, cis-3-(3′, 4′-dimethoxyphenyl)-4-[(E)-3‴, 4‴-dimethoxystyryl] cyclohex-1-ene, exhibits apoptogenic properties in T-acute lymphoblastic leukemia cells via induction of p53-independent mitochondrial signalling pathway. *Evid-Based Compl Alt.* 2013;2013.
30. Lövborg H, Nygren P, Larsson R. Multiparametric evaluation of apoptosis: effects of standard cytotoxic agents and the cyanoguanidine CHS 828. *Mol Cancer Ther.* 2004;3(5):521–526.
31. Suvitha Syama, Ahmad Bustamam, Rasedee Abdullah, et al. b-Mangostin induces p53-dependent G2/M cell cyclearrest and apoptosis through ROS mediated mitochondrial pathway and NfkB suppression in MCF-7 cells. *J Funct Foods.* 2014;6:290–304.
32. Taylor JL, Elgorashi EE, Maes A, et al. Investigating the safety of plants used in South African traditional medicine: testing for genotoxicity in the micronucleus and alkaline comet assays. *Environ Mol Mutagen.* 2003;42(3):144–154.
33. de Sá Ferreira IC, Ferrão Vargas VM. Mutagenicity of medicinal plant extracts in Salmonella/microsome assay. *Phytother Res.* 1999;13(5):397–400.

34. Li JW, Vederas JC. Drug discovery and natural products: end of an era or an endless frontier? *Science*. 2009;325(5937):161–165.

35. Deb DD, Parimala G, Saravana Devi S, Chakraborty T. Effect of thymol on peripheral blood mononuclear cell PBMC and acute promyelotic cancer cell line HL-60. *Chem Biol Interact*. 2011;193(1):97–106.

36. Arunasree KM. Anti-proliferative effects of carvacrol on a human metastatic breast cancer cell line, MDA-MB 231. *Phytomedicine*. 2010;17(8–9):581–588.

37. Yin QH, Yan FX, Zu XY, et al. Anti-proliferative and pro-apoptotic effect of carvacrol on human hepatocellular carcinoma cell line HepG-2. *Cytotechnology*. 2012;64(1):43–51.

38. Koparal AT, Zeytinoglu M. Effects of Carvacrol on a Human Non-Small Cell Lung Cancer (NSCLC) Cell Line, A549. *Cytotechnology*. 2003;43(1–3):149–154.

39. Lakhani SA, Masud A, Kuida K, et al. Caspases 3 and 7: key mediators of mitochondrial events of apoptosis. *Science*. 2006;311(5762):847–851.

40. Ocker M, Höpfner M. Apoptosis-modulating drugs for improved cancer therapy. *Eur Surg Res*. 2012;48(3):111–120.

41. Zhang G, Gurtu V, Kain SR, Yan G. Early detection of apoptosis using a fluorescent conjugate of annexin V. *Biotechniques*. 1997;23(3):525–531.

42. Koopman G, Reutelingsperger CP, Kuijten GA, Keehnen RM, Pals ST, van Oers MH. Annexin V for flow cytometric detection of phosphatidylserine expression on B cells undergoing apoptosis. *Blood*. 1994;84(5):1415–1420.

43. Edinger AL, Thompson CB. Death by design: apoptosis, necrosis and autophagy. *Curr Opin Cell Biol*. 2004;16(6):663–669.

44. Pantalacci S, Tapon N, Léopold P. The Salvador partner Hippo promotes apoptosis and cell-cycle exit in Drosophila. *Nat Cell Biol*. 2003;5(10):921–927.

45. Vermeulen K, Berneman ZN, Van Bockstaele DR. Cell cycle and apoptosis. *Cell Prolif*. 2003;36(3):165–175.

46. Imreh G, Norberg HV, Imreh S, Zhivotovsky B. Chromosomal breaks during mitotic catastrophe trigger γH2AX-ATM-p53-mediated apoptosis. *J Cell Sci*. 2011;124(Pt 17):2951–2963.

47. Pucci B, Kasten M, Giordano A. Cell cycle and apoptosis. *Neoplasia*. 2000;2(4):291–299.

48. Fan TJ, Han LH, Cong RS, Liang J. Caspase family proteases and apoptosis. *Acta Biochim Biophys Sin (Shanghai)*. 2005;37(11):719–727.

49. Karmakar S, Banik NL, Patel SJ, Ray SK. Curcumin activated both receptor-mediated and mitochondria-mediated proteolytic pathways for apoptosis in human glioblastoma T98G cells. *Neurosci Lett*. 2006;407(1):53–58.

50. Karunagaran D, Rashmi R, Kumar TR. Induction of apoptosis by curcumin and its implications for cancer therapy. *Curr Cancer Drug Targets*. 2005;5(2):117–129.

51. Würstle ML, Laussmann MA, Rehm M. The central role of initiator caspase-9 in apoptosis signal transduction and the regulation of its activation and activity on the apoptosome. *Exp Cell Res*. 2012;318(11):1213–1220.

52. Reed JC. Bcl-2 family proteins. *Oncogene*. 1998;17(25):3225–3236.

53. Vaseva AV, Marchenko ND, Ji K, Tsirka SE, Holzmann S, Moll UM. p53 opens the mitochondrial permeability transition pore to trigger necrosis. *Cell*. 2012;149(7):1536–1548.

54. Suzuki Y, Imai Y, Nakayama H, Takahashi K, Takio K, Takahashi R. A serine protease, HtrA2, is released from the mitochondria and interacts with XIAP, inducing cell death. *Mol Cell*. 2001;8(3):613–621.

55. Kim HS, Ingermann AR, Tsubaki J, Twigg SM, Walker GE, Oh Y. Insulin-like growth factor-binding protein 3 induces caspase-dependent apoptosis through a death receptor-mediated pathway in MCF-7 human breast cancer cells. *Cancer Res*. 2004;64(6):2229–2237.

56. Nagata S. Apoptosis by death factor. *Cell*. 1997;88(3):355–365.

57. Verlinden L, Verstuyf A, Convents R, Marcelis S, Van Camp M, Bouillon R. Action of 1,25(OH)2D3 on the cell cycle genes, cyclin D1, p21 and p27 in MCF-7 cells. *Mol Cell Endocrinol*. 1998;142(1–2):57–65.

58. Coqueret O. New roles for p21 and p27 cell-cycle inhibitors: a function for each cell compartment? *Trends Cell Biol*. 2003;13(2):65–70.

59. Esposito L, Indovina P, Magnotti F, Conti D, Giordano A. Anticancer therapeutic strategies based on CDK inhibitors. *Curr Pharm Des*. 2013;19(30):5327–5332.

Supplementary material

Table S1 Serum biochemical analysis of rats

A

Animal groups	Kidney function test						
	Sodium (mM/L)	Potassium (mM/L)	Chloride (mM/L)	Co_2 (mM/L)	Anion gap (mM/L)	Urea (mM/L)	Creatinine (μM/L)
Vehicle	138.66±0.76	3.7±0.01	100.21±0.33	25.9±0.44	13.3±0.56	5.32±0.47	32.15±1.76
FALHE (2 g/kg)	142.21±0.51	4.1±0.3	101.24±0.4	27.78±0.98	15.5±0.64	6.13±0.54	30.21±1.27
FALHE (5 g/kg)	140.21±0.77	4.0±0.02	105.27±0.33	25.26±0.8	16.15±0.44	6.99±0.29	30.15±1.19

B

Animal groups	Liver function test							
	Total protein (g/L)	Albumin (g/L)	Globulin (g/L)	TB (μmol/L)	AP (U/L)	ALT (U/L)	AST (U/L)	GGT (U/L)
Vehicle	70.6±1.6	39.9±0.9	29.7±1.8	1.1±0.05	161.5±5.7	30.9±1.4	24.2±2.8	0.45±0.07
FALHE (2 g/kg)	67.9±1.8	38.5±0.3	30.6±1.2	1.4±0.06	163.8±4.1	35.5±1.7	25.48±2.9	0.57±0.09
FALHE (5 g/kg)	69.7±1.6	38.7±0.9	31.5±1.5	1.4±0.04	163.3±5.2	36.7±1.8	27.7±4.2	0.6±0.03

C

Animal Groups	Hematological test								
	HGB (g/dL)	HCT (%)	RBC (10^6 cells/μL)	MCV (fL)	MCH (pg)	MCHC (g/dL)	RDW (%)	WBC (10^3/μL)	Platelet (10^3/μL)
Vehicle	16.03±0.7	39±0.00	9.3±0.1	60.2±0.5	17.5±0.3	33.34±0.7	14.1±0.4	6.2±0.4	999.5±32.5
FALHE (2 g/kg)	16.27±0.9	39±0.00	9.4±0.2	61.4±0.6	16.9±0.6	33.01±0.5	12.23±0.1	6.0±0.3	975.3±35.2
FALHE (5 g/kg)	16.38±0.2	38±0.00	9.3±0.1	59.8±0.7	15.9±0.9	32.93±0.9	12.7±0.4	5.9±0.2	969.2±23.8

Notes: Serum biochemical analysis of rats did not show any sign of FALHE toxicity on (**A**) renal function test, (**B**) liver function test, and (**C**) hematological parameters of the rodents, when compared with the control group. Values expressed as mean±standard deviation.
Abbreviations: ALT, alanine aminotransferase; AST, aspartate aminotransferase; AP, alkaline phosphatase; GGT, G-glutamyl transferase; HCT, hematocrit; HGB, hemoglobin; MCH, mean corpuscular hemoglobin; MCHC, mean corpuscular hemoglobin concentration; MCV, mean corpuscular volume; RBC, red cell count; RDW, red cell distribution width; TB, total bilirubin; WBC, white cell; FALHE, *Ferulago angulata* leaves hexane extract.